Nature of Ho Magnetism in Multiferroic HoMnO$_3$

S. Nandi,[1] A. Kreyssig,[1] L. Tan,[1] J. W. Kim,[1] J. Q. Yan,[1] J. C. Lang,[2] D. Haskel,[2] R. J. McQueeney,[1] and A. I. Goldman[1]

[1]*Ames Laboratory, US DOE, and Department of Physics and Astronomy, Iowa State University, Ames, Iowa 50011, USA*
[2]*Advanced Photon Source, Argonne National Laboratory, Argonne, Illinois 60439, USA*

Using x-ray resonant magnetic scattering and x-ray magnetic circular dichroism, techniques that are element specific, we have elucidated the role of Ho^{3+} in multiferroic HoMnO$_3$. In zero field, Ho^{3+} orders antiferromagnetically with moments aligned along the hexagonal **c** direction below 40 K, and undergoes a transition to another magnetic structure below 4.5 K. In applied electric fields of up to 1×10^7 V/m, the magnetic structure of Ho^{3+} remains unchanged.

Magnetoelectric multiferroic compounds, systems which exhibit both ferroelectric and magnetic effects within the same phase, have attracted considerable attention due to the potential for controlling electric polarization by an applied magnetic field [1] or, conversely, magnetic order through an applied electric field [2]. Recently, such a mechanism has been proposed for hexagonal HoMnO$_3$ [2]. Despite numerous studies, however, the exact role that the Ho^{3+} ions play in the magnetic response, and the details of the magnetic ordering of the Ho^{3+} sublattices remain unclear [3–8].

Below $T_C = 875$ K, the ferroelectric phase of HoMnO$_3$ possesses $P6_3cm$ symmetry and a polarization $P_C = 5.6 \ \mu C/cm^2$ along the hexagonal **c** axis [9]. The Mn^{3+} moments order antiferromagnetically within the **a**-**b** plane below the Néel temperature, $T_N = 76$ K, and undergo reorientation transitions at approximately 40 and 5 K [5,10]. There have been several investigations of the role of Ho^{3+} in the magnetic ordering of this compound, but with contradictory results. For clarity in the discussion that follows, we list the various magnetic symmetries and their features in Table I and refer to the associated magnetic configurations for Ho^{3+} by their magnetic representation.

Muñoz *et al.* [7] proposed that the magnetic representation is Γ_1 in the temperature range 24.6 to 1.7 K based upon neutron powder diffraction measurements. Lonkai *et al.* [6] and Fiebig *et al.* [4,5] proposed that from 40 to 5 K the magnetic representation is Γ_3 and transforms, below 5 K, to Γ_1 based on neutron diffraction experiments and optical second harmonic generation (SHG) experiments, respectively. Most recently, Brown and Chatterji [8] claimed that the magnetic representation is Γ_3 from 40 K down to 2 K based on neutron diffraction on single crystals and powders. All of the above studies concluded that the Ho^{3+} moments order along the hexagonal **c** axis. In their analysis of magnetoelectric measurements, however, Sugie *et al.* [3] proposed that the Ho^{3+} moments order noncollinearly in the hexagonal **a**-**b** plane. Perhaps of strongest interest is the proposal by Lottermoser *et al.* [2] that the application of an electric field changes the antiferromagnetic order of Ho^{3+} to ferromagnetic order, with the representation Γ_2,

over the temperature range from 2 to 76 K, based on SHG and optical Faraday rotation experiments.

To resolve the contradictions regarding the magnetic order of Ho^{3+} below 40 K in zero field, and to investigate the nature of the Ho^{3+} magnetic ordering in an applied electric field, we have performed x-ray resonant magnetic scattering (XRMS) and x-ray magnetic circular dichroism (XMCD) studies of HoMnO$_3$ at the Ho L_{III} absorption edge ($E = 8.071$ keV). In the XRMS experiment, the scattering process involves an intermediate state which arises from either dipole ($E1$) allowed ($2p$–$5d$) or quadrupole ($E2$) allowed ($2p$–$4f$) electronic excitations [11,12]. In ordered rare-earth magnetic materials, the technique is sensitive to the magnetization density through either the $4f$ electronic states directly ($E2$) or indirectly through the $4f$–$5d$ exchange interaction ($E1$). Of importance here is that since this technique is element specific, we can probe the magnetic structure associated with the Ho^{3+} moments directly. In the closely related XMCD measurements, the signal is defined as the difference in the absorption of circularly polarized x rays with the helicity parallel and antiparallel to the sample magnetization [13]. Since XMCD measurements are also performed at the absorption edges of elements of interest, they can be viewed as measurements of the net magnetization for a specific elemental constituent of a magnetic compound, for example, measuring the contribution of Ho^{3+} to any ferromagnetic response of the sample.

Single crystals of HoMnO$_3$ were grown using a floating zone method and prepared with a polished surface perpendicular to the crystallographic **c** axis. The magnetic properties (e.g. details of the complex magnetic phase diagram) agree well with reported results [10,14]. The XRMS experiment was performed on the 6ID-B beam line at the Advanced Photon Source at the Ho L_{III} absorption edge. The sample was mounted on the cold-finger of a displex cryogenic refrigerator with the **a***-**c*** reciprocal plane coincident with the scattering plane. With the incident beam polarized perpendicular to the scattering plane (σ-polarized), measurements of the magnetic scattering were performed at the $E1$ and $E2$ resonances in the rotated

TABLE I. Magnetic representations for HoMnO$_3$ according to Refs. [2,7] for moments along the **c** direction. Additional magnetic representations, Γ_5 and Γ_6, allow moments only in the **a**-**b** plane and only Γ_6 yields magnetic intensity for (0 0 l) and (h 0 l) reflections with l odd. The atomic positions for Ho are given in brackets. [z, $+$, $-$] depict $z_{2a} = 0.273$, $+\mu_{2a}^c$, $-\mu_{2a}^c$, and $z_{4b} = 0.231$, $+\mu_{4b}^c$, $-\mu_{4b}^c$ for the Wyckoff sites Ho (2a) and Ho (4b), respectively [7]. The symbol [0] labels no ordered magnetic moment at this site.

	Ho (2a)		Ho (4b)				Magnetic intensity	
Magnetic representation	$\begin{pmatrix} 0 \\ 0 \\ z \end{pmatrix}$	$\begin{pmatrix} 0 \\ 0 \\ z+1/2 \end{pmatrix}$	$\begin{pmatrix} 1/3 \\ 2/3 \\ z \end{pmatrix}$	$\begin{pmatrix} 2/3 \\ 1/3 \\ z \end{pmatrix}$	$\begin{pmatrix} 1/3 \\ 2/3 \\ z+1/2 \end{pmatrix}$	$\begin{pmatrix} 2/3 \\ 1/3 \\ z+1/2 \end{pmatrix}$	(0 0 l), l odd	(h 0 l), l odd
Γ_1	0	0	+	−	−	+	no	yes
Γ_2	+	+	+	+	+	+	no	no
Γ_3	+	−	+	+	−	−	yes	yes
Γ_4	0	0	+	−	+	−	no	no

($\sigma - \pi$) scattering channel [15]. Pyrolytic graphite (0 0 6) was used as a polarization analyzer to suppress the charge background (unrotated) relative to the magnetic scattering signal. The XMCD measurements were performed on the 4ID-D beam line at the Advanced Photon Source by modulating the x-ray helicity at 11.3 Hz with a thin diamond phase retarder and using a lock-in amplifier to detect the related modulation in the absorption coefficient. Spectra were recorded from a 20 μm thin single crystal coated with carbon as electrodes and on a powder sample spread over several layers of tape and then sandwiched between two layers of conducting aluminized mylar (total sandwich thickness of 280 μm). The samples were mounted on the cold finger of a horizontal field cryomagnet.

We first turn our attention to the magnetic structure of Ho^{3+} in the absence of an applied electric field. Figure 1(a) shows energy scans through the Ho L_{III} absorption edge at the (0 0 9) reciprocal lattice point which is forbidden for charge scattering. Below 39 K, we observed two resonance peaks which correspond to the quadrupole resonance (just below the Ho L_{III} absorption edge) and the dipole resonance (just above the Ho L_{III} absorption edge). Recent XRMS work on TbMnO$_3$ [16], has shown that resonant scattering features can involve both charge and magnetic contributions in the more complex perovskite multiferroic compounds. In hexagonal HoMnO$_3$, the predominant magnetic origin of the resonant scattering is supported by the following points. First, we note the close proximity in energy between the XRMS resonances [Fig. 1(a)] and the quadrupole and dipole features in the XMCD spectrum of the powder sample in an applied magnetic field of 0.4 Tesla [Fig. 1(b)]. The magnetic origin of the XMCD features was confirmed by the observation that the spectrum flips upon reversal of the applied magnetic field. In addition, fits to the XRMS integrated intensities for (0 0 l) (l odd) diffraction peaks measured at each resonance are consistent with the expected angular and polarization dependence of the dipole and quadrupole resonant scattering cross sections, respectively [15,17,18].

Figure 2 shows the measured peak intensities for two characteristic magnetic reflections, (0 0 9) and (1 0 9), as a function of temperature from 1.7 K to 45 K. Also shown

are the integrated intensities measured in θ-scans (rocking scans) at several temperatures for the (0 0 9) reflection. Because of strong local heating effects from the incident beam, significant attenuation of the undulator beam ($\geq 98\%$) was required to accurately measure the temperature dependence over the entire temperature range. Above $T = 39$ K, we find no signal at these magnetic peak positions. Just below 39 K there is an abrupt increase in both the dipole and quadrupole diffraction peak intensities, followed by a smooth increase with decreasing temperature down to 4.5 K. The temperature of the onset of magnetic Ho^{3+} ordering agrees well with the kink in magnetization data and the Mn^{3+} spin reorientation transition as found by Vajk *et al.* [10]. At 4.5 K, changes in the intensities of the (0 0 9) and (1 0 9) magnetic peaks signal a change in the magnetic ordering of Ho^{3+} in this low temperature phase (LTP), from the intermediate temperature phase (ITP) for 4.5 K $< T <$ 39 K.

To determine the moment direction in the intermediate phase, we measured the intensity of the off-specular reflections, (3 0 9) and ($\bar{3}$ 0 9), at $T = 12$ K. While the magnetic structure factor is the same for both reflections, the angular dependence of the dipole resonant scattering cross section [15] is different providing strong sensitivity to the moment direction. The experimentally observed intensity ratio $I(3\,0\,9)/I(\bar{3}\,0\,9)$ is 76 $\pm$ 14. For the Ho^{3+} moment oriented along the hexagonal **c** axis, the calculated intensity ratio $I(3\,0\,9)/I(\bar{3}\,0\,9) = 86.3$, while for moments lying in the **a**-**b** plane, $I(3\,0\,9)/I(\bar{3}\,0\,9) = 0.32$. Thus, within experimental error, the Ho^{3+} moments lie along the hexagonal **c** axis.

As identified in previous work, the magnetic unit cell is the same as the chemical unit cell [7]. In order to determine the appropriate magnetic representation [19] we must look into details of the six magnetic representations that are possible for the crystallographic space group $P6_3cm$, listed in Ref. [7]. Only four magnetic representations (from Γ_1 to Γ_4) are compatible with Ho^{3+} magnetic moments along the hexagonal **c** direction and are described in Table I. From the last columns of Table I, we see that only the magnetic representation Γ_3 yields nonzero intensity for (0 0 l) reflections with l odd. While details will be presented else-
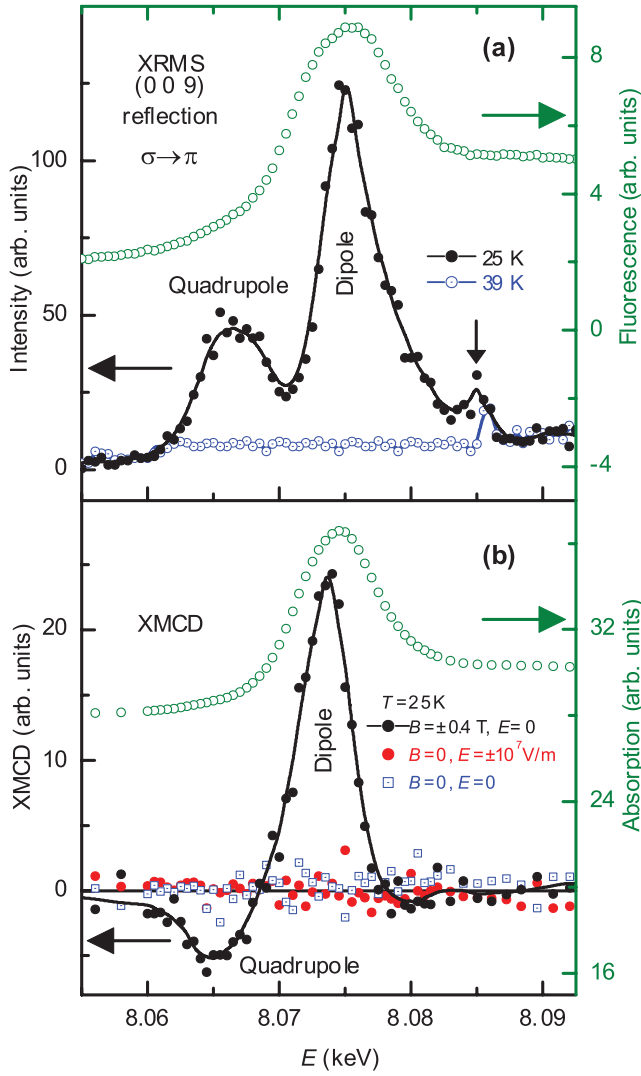
FIG. 1 (color). (a) Energy scans for the magnetic (0 0 9) reflection and the fluorescence spectra through the Ho L_{III} absorption edge. The solid lines are guides to the eye. The small peak marked by a vertical arrow is due to multiple charge scattering. (b) The XMCD and absorption spectra at the Ho L_{III} edge with applied magnetic, electric fields and without any fields, measured on a powder sample at 4ID-D. The solid line is a guide to the eye.

where [17], here we note that at 6 K, the measured integrated intensities of a series of (0 0 l) reflections are consistent with calculated values for both dipole and quadrupole resonant scattering based on the magnetic representation Γ_3 and yields an ordered magnetic moment for the Ho (2a) site twice that of the Ho (4b) site at 6 K.

The temperature dependence of the Ho^{3+} XRMS signal in the ITP [as shown in Fig. 2(a)] exhibits a concave curvature quite similar to what was observed in XRMS measurements of orthorhombic multiferroic $DyMnO_3$, and ascribed to the induced magnetic ordering of Dy^{3+} [20]. For hexagonal $HoMnO_3$, this behavior may be explained with reference to other systems with ground state quasi-
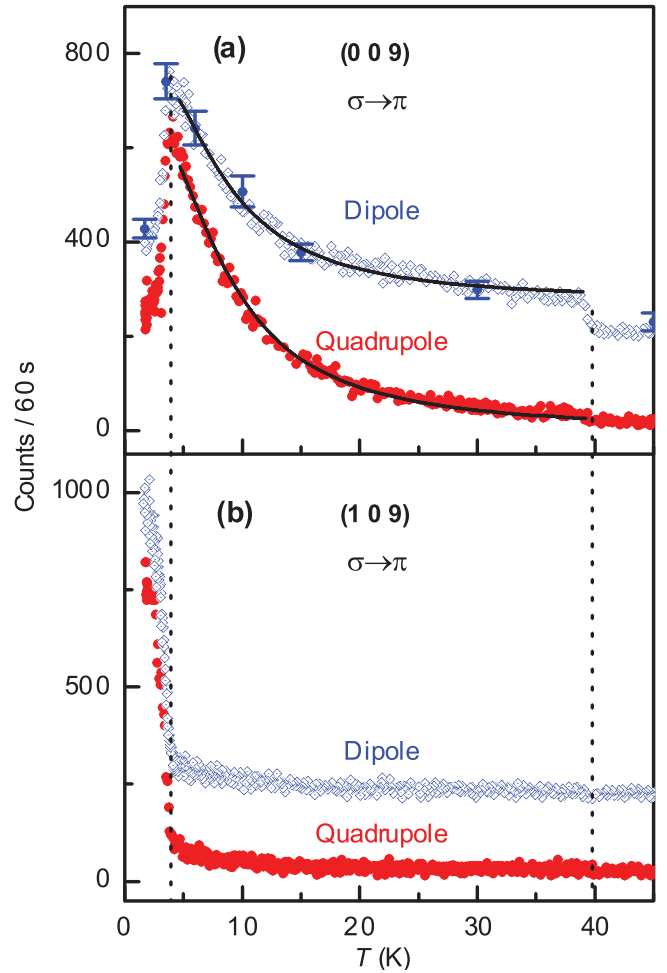
FIG. 2 (color). Temperature dependence of the magnetic peak intensity for the (0 0 9) and (1 0 9) reflections, measured for both the dipole and quadrupole resonances. The dipole resonance data are vertically displaced for clarity. Solid blue circles represent the integrated intensity of peaks measured at selected temperatures. The solid black lines are fits to the data in the intermediate magnetic phase as described in the text.

doublet crystal field levels, split by an exchange field [21–23]. The non-Kramers Ho^{3+} ions in $HoMnO_3$ are at positions of trigonal symmetry which typically leads to singlets with very small zero-field splitting, forming such a quasi-doublet [24,25]. As a first attempt, if we assume an effective two level system with a splitting Δ_{eff}, the temperature dependence in the ITP, should goes as $(\tanh\frac{\Delta_{eff}}{2kT})^2$ [21,22]. Fits to the temperature dependence of the dipole and quadrupole resonant scattering in the ITP yields $\Delta_{eff} = (1.3 \pm 0.2)$ meV, consistent with the low-energy crystal electric field transition of Ho^{3+} of 1.5 meV observed in neutron scattering measurements below 40 K [10,26]. The ordering at the Ho^{3+} sites in the ITP may be induced by changes in the anisotropic superexchange interactions resulting from the reorientation of the Mn^{3+} moments [27].

We now turn to our investigation of the magnetic structure of the LTP. From Fig. 2 we see that the intensity of
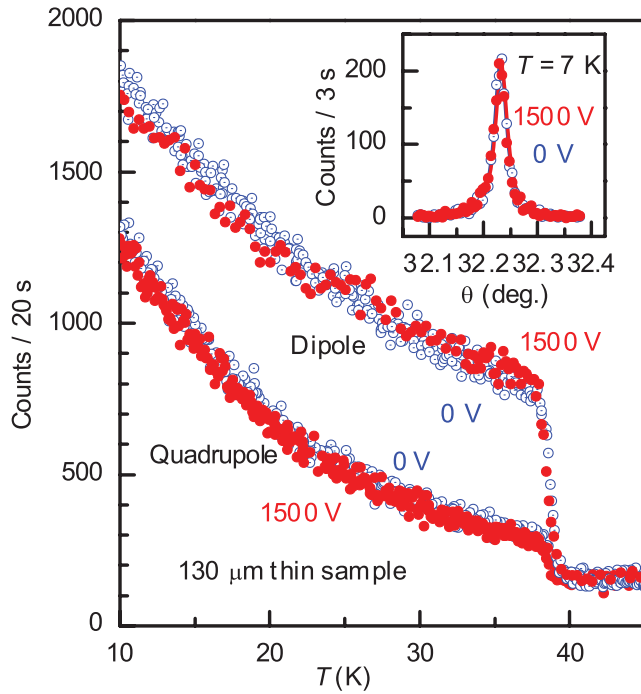
FIG. 3 (color). Effect of an applied electric field on the (0 0 9) antiferromagnetic peak. Inset: rocking scans at 0 and 1500 V for the quadrupole resonance at 7 K.

(0 0 9) decreases while the intensity of (1 0 9) increases strongly below 4.5 K. Similar to our approach for the ITP, we confirmed that the moments lie primarily along the **c** axis by measuring the integrated intensities of the $(2\ 0\ 9)$ and $(\bar{2}\ 0\ 9)$ reflections at 2 K. The decrease in intensity for the (0 0 9) reflection and increase in the (1 0 9) reflection signal a transition from Γ_3 to Γ_1 (see Table I). An interesting consequence of this transition is that the Ho (2a) site cannot order magnetically according to the representation Γ_1. The finite intensity of the (0 0 9) reflection below 4.5 K is likely due to residual beam heating effects although we can not exclude a mixed Γ_3/Γ_1 phase in this region.

After determining the magnetic structure in zero field, we measured the temperature dependence of both dipole and quadrupole resonances in an applied electric field. For these measurements, a thinned (130 μm) sample coated with silver (as electrodes) was used. Fields of up to 1×10^7 V/m, well above the saturation value reported by Lottermoser et al. [2], were obtained for an applied voltage of 1500 V. Figure 3 shows that there is no difference between the temperature dependence of the peak intensity in zero and the maximum applied electric field. Further, the inset to the Fig. 3 shows that there are no gross structural changes in this applied field since the peak position and the full width at half maximum remain same. We conclude that there is no change of the antiferromagnetic structure of Ho^{3+} in an applied electric field in the ITP.

Since the XRMS measurements probe only antiferromagnetic order and are not sensitive to small ferromagnetic components of the ordered magnetic moment, we have performed XMCD measurements, at the Ho L_{III} edge, on single crystal and powder samples. As illustrated for the powder sample in Fig. 1(b), the XMCD signal is unaffected by applied electric fields of up to approximately 1×10^7 V/m for either sample, for temperatures between 8 and 80 K. We conclude that Ho^{3+} is not responsible for the reported ferromagnetic response of $HoMnO_3$ in an applied electric field.

Note added in proof.—It has come to our attention that neutron diffraction measurements also observe no change in magnetic order in applied electric fields [28].

[1] T. Kimura *et al.*, Nature (London) **426**, 55 (2003).
[2] T. Lottermoser *et al.*, Nature (London) **430**, 541 (2004).
[3] H. Sugie *et al.*, J. Phys. Soc. Jpn. **71**, 1558 (2002).
[4] M. Fiebig *et al.*, J. Appl. Phys. **91**, 8867 (2002).
[5] M. Fiebig *et al.*, Phys. Rev. Lett. **84**, 5620 (2000).
[6] T. Lonkai *et al.*, Appl. Phys. A **74**, S843 (2002).
[7] A. Muñoz *et al.*, Chem. Mater. **13**, 1497 (2001).
[8] P. J. Brown and T. Chatterji, J. Phys. Condens. Matter **18**, 10 085 (2006).
[9] P. Coeuré *et al.*, in *Proc. of 1st Intl. Meeting on Ferroelectricity* (Institute of Physics, Czech. Acad. Sci., Prague, 1966), p. 332.
[10] O. P. Vajk *et al.*, Phys. Rev. Lett. **94**, 087601 (2005).
[11] D. Gibbs *et al.*, Phys. Rev. Lett. **61**, 1241 (1988).
[12] J. P. Hannon *et al.*, Phys. Rev. Lett. **61**, 1245 (1988).
[13] J. C. Lang, in *Methods in Materials Research: A Current Protocols Publication*, edited by E. N. Kaufmann (J. Wiley & Sons, New York, 2000), Chap. 10c2.
[14] B. Lorenz *et al.*, Phys. Rev. B **71**, 014438 (2005).
[15] J. P. Hill and D. F. McMorrow, Acta Crystallogr. Sect. A **52**, 236 (1996).
[16] D. Mannix *et al.*, Phys. Rev. B **76**, 184420 (2007).
[17] S. Nandi *et al.* (unpublished).
[18] C. Detlefs *et al.*, Phys. Rev. B **55**, R680 (1997).
[19] E. F. Bertaut, Acta Crystallogr. Sect. A **24**, 217 (1968).
[20] O. Prokhnenko *et al.*, Phys. Rev. Lett. **98**, 057206 (2007).
[21] M. N. Popova *et al.*, Phys. Rev. B **71**, 024414 (2005).
[22] R. Sachidanandam *et al.*, Phys. Rev. B **56**, 260 (1997).
[23] A. Zheludev *et al.*, Phys. Rev. B **54**, 7216 (1996).
[24] U. Ranon and K. Lee, Phys. Rev. **188**, 539 (1969).
[25] V. Hardy *et al.*, Phys. Rev. B **74**, 064413 (2006).
[26] H. D. Zhou *et al.*, Phys. Rev. B **74**, 094426 (2006).
[27] M. Fiebig *et al.*, Phys. Rev. Lett. **88**, 027203 (2001).
[28] J. W. Lynn, private communication.